Fringe-tracking experiments at the IOTA interferometer

S. Morel[a], W. A. Traub[b], J. D. Bregman[c], R. Mah[c], and E. Wilson[c]

[a]Smithsonian Astrophysical Observatory - F. L. Whipple Observatory
670 Mount-Hopkins Road, Amado, AZ 85645, USA

[b]Smithsonian Astrophysical Observatory - Center for Astrophysics
60 Garden Street, Cambridge, MA 02138, USA

[c]NASA - Ames Research Center, MS 245-6
Moffet-Field, CA 94035, USA

ABSTRACT

Keywords: fringe-tracking, coherencing, infrared detectors, precision positioning, prediction.

1. INTRODUCTION

A two-aperture stellar optical interferometer is always subject, while being operated, to variations of the optical path difference (OPD) between the two light beams coming from its telescopes. One of the OPD variation components is a deterministic signal related to Earth rotation. It is compensated by moving an optical delay line (ODL) according to a pointing model given by the declination of the observed object and its hour angle. The other components are random signal caused by atmospheric turbulence ("differential piston" mode of the turbulence), mechanical constraints, vibrations, errors in the pointing model. Interference fringes are observable within an OPD interval roughly equal to the coherence length defined by $L_c = \bar{\lambda}^2/\Delta\lambda$, where $\bar{\lambda}$ is the mean wavelength and $\Delta\lambda$ is the spectral interval.

The aim of fringe-tracking is to perform a real-time correction of the length difference between the actual null-OPD position and the expected null-OPD position, in order to keep observing fringes. This difference is computed from the fringe signal acquired and is used to control an optical delaying device. In order to not "share the photons", the fringe-tracker uses directly the "scientific" fringes acquired for measuring either their contrast yielding visibility points (imaging interferometry) or external delay (in case of astrometry by interferometry). However, in some cases, it may be useful to have separated recombiners for acquisition and tracking[1].

Although it is possible to manually track the fringes (see part 3), significant fringe acquisition improvements are expected from an automatic fringe-tracker. The implementation of a fringe-tracker depends on the way fringes are acquired. With channeled spectrum (for small apertures) or dispersed fringes (for apertures larger than Fried's parameter r_0) configurations, one can track fringes by respectively group-delay tracking[2] (GDT) or real-time active fringe tracking[3] (RAFT). However, no photon-counting technology currently exists for infrared: the fringe signal-to-noise ratio decreases with the number of pixels of the detector. The signal should be therefore "concentrated" on a minimal number of pixels. The classical "white- fringe" set-up is then employed (Fig. 1). The two beams are recombined by a beamsplitter. Fringes are acquired by linearly modulating (by a sawtooth signal ideally) the pathlength of any of the beam upstream the recombination. Intensities of the recombined beams evolve therefore

Further author information:

S.M.: E-mail: smorel@cfa.harvard.edu. Fax: 1 520 670 5751

W.A.T.: E-mail: wtraub@cfa.harvard.edu. Fax:1 617 495 7105

J.D.B.: E-mail: jbregman@mail.arc.nasa.gov

R.M.: E-mail: rmah@mail.arc.nasa.gov

E.W.: E-mail: ed.wilson@ibm.net

temporally as an interference fringe pattern. Due to reflections on the beamsplitter, there is a π phase-shift between the two interferometric signals obtained.

The pathlength scanned depends on the detector performances and is usually equal to a few coherence lengths. For a white-fringe set-up, one can perform "cophasing" in order to "freeze" fringes moved by atmospheric differential piston[4]. However, a very good fringe SNR is necessary for this technique. A less demanding way to perform fringe-tracking is called "coherencing": the OPD is corrected to remain within the "observing window" defined by the scan length. Group-delay tracking and RAFT may be regarded as coherencing techniques. For any set-up, the OPD correction rate is between 0.2 Hz and 10 Hz. The duration of a cycle is therefore longer than the atmospheric τ_0.

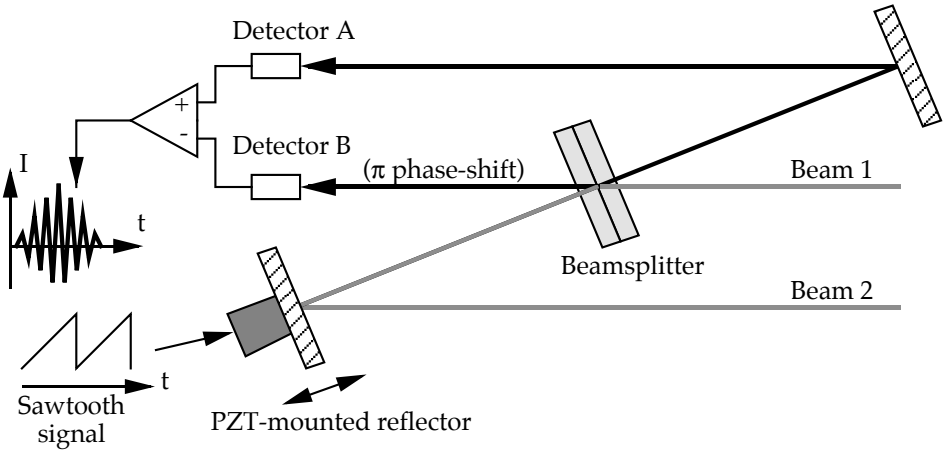

Figure 1. Schematic of a recombination table based on a beamsplitter, as it is employed on IOTA for fringe acquisition.

2. COHERENCING ALGORITHM

With a white-fringe set-up, the two interferometric signals resulting from a scan are subtracted to yield an interferogram. For each interferogram (or fringe packet) acquired, the computer performing fringe-tracking finds the null-OPD point and computes the offset to apply to the delaying device, in order to bring the null-OPD point at the center of the observing window (i.e., half-way on the scan length).

For IOTA (see part 3), fringe packet values are temporally sampled on 256 points. Each value is a 16-bit integer. We use the following algorithm to find the null-OPD point in a fringe packet:

1) The photometric variations are removed by subtracting to each value of the fringe packet its local mean (computed from the values of the 20 points closest to a given point). A bandpass filtering by FFT can be used instead, and gives satisfying results.
2) The negative values of the signal obtained are multiplied by -1 (equivalent of a rectifier bridge).
3) All the values that are not local maxima are set to zero.
4) Linear segments are interpolated between each pair of non-zero points (corresponding to fringe peaks in the interferogram).
5) The obtained signal is smoothed by a "schematized" coherence envelope given by flat-top functions representing the main lobe and two sidelobes. The location of the maximum value in the signal resulting from the previous operation gives the null-OPD point.

These steps are illustrated by Fig. 2. This algorithm is actually a simplified version of a first one that included phase measurement. It algorithm was first tested in MatLab language using recorded interferograms. A good robustness to noise was noticed. Tests were also done using simulated interferograms: the RMS error on the null-OPD point found is never larger than 20 points. With the IOTA fringe acquisition system (see part 3), this corresponds to an error on the estimated null-OPD point of 8 μm, very satisfying for a coherencing system.

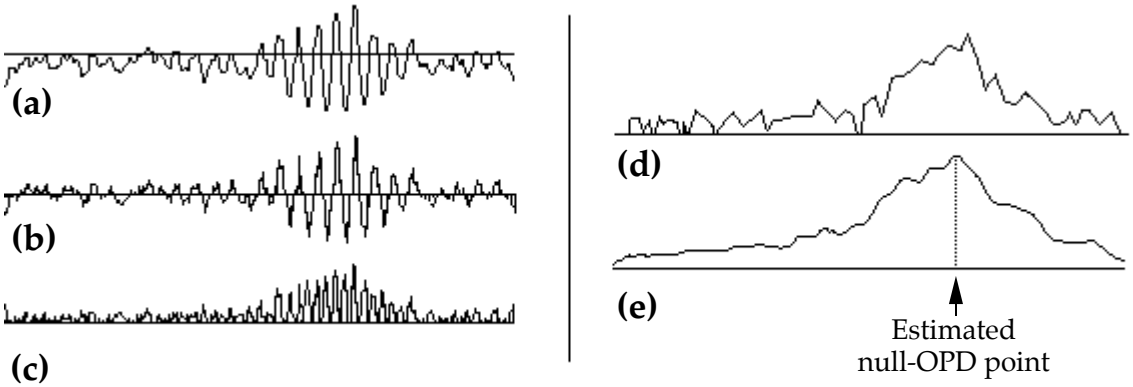

Figure 2. Illustration of the steps of the coherencing algorithm. (a): Interferogram acquired ; (b): signal obtained from this interferogram after step 1 (correction of the photometric variations) ; (c): signal obtained after step 2 (rectification) ; (d): signal obtained after steps 3 and 4 ; (d): signal obtained after step 5 (smoothing). The null-OPD point corresponds to the position of the maximum value in this signal.

3. FRINGE-TRACKER IMPLEMENTATION ON THE IOTA INFRARED TABLE

IOTA can currently use either a single-mode fiber recombiner called FLUOR[5] or a beamsplitter-based recombiner, as described by Fig. 1. For scanning the OPD, a plane mirror is mounted on a piezo-electric transducer (PZT) which is controlled by a triangle signal generated by a low-frequency analog function generator. Our fringe-tracker has been designed for this recombiner only. The detector used for fringe acquisition is based on a 128×128 pixel NICMOS III chip[6]. Only two pixels of this chip are read for acquiring interferometric signals. The maximum rate $f_s = 1/\tau_s$ is 10 interferograms per second, each one being 256 point wide. The NICMOS chip is controlled by signals generated by a Pentium 100 MHz PC which receives the sampled value of the addressed pixel. After processing, these values are sent to a Macintosh Quadra computer displaying and recording interferograms acquired.

The delaying device used by IOTA for compensating the OPD due to Earth rotation is the "short ODL". It consists of a dihedral reflector mounted on an Anorad micro-positioning table. This table may be translated within a 2.3 m interval by 10 nm steps thanks to an electric linear motor featuring a position servo-loop by laser metrology. The short ODL is controlled by another Macintosh Quadra. Without fringe-tracker, the operator has to check the position of the interferogram displayed by the first Quadra and manually modify the short ODL position from the second Quadra to keep the fringe packet observable. This operation is difficult when the turbulence is important. Implementing an automatic coherencer fringe-tracking system would therefore significantly improve data acquisition on IOTA.

To implement the fringe-tracker, the algorithm described in part 2 was coded in C++ language for a temporary Macintosh PowerBook (100 MHz PowerPC CPU). The interferogram acquisition and ODL control programs were modified to communicate with the fringe-tracker computer: each interferogram is sent through the Ethernet local area network (LAN) of IOTA to the fringe-tracker. After having found the null-OPD point in the interferogram, the fringe-tracker computer sends the OPD correction to the ODL control computer which adjusts the short ODL position.

Some problems were encountered during the test of this first version of the IOTA fringe-tracker. The TCP/IP protocol used for communication between the computers is not suitable for our real-time application involving MacOS computers. Hence, we now use UDP (User Datagram Protocol) which is a socket-based protocol faster and more flexible than TCP/IP, for all the IOTA applications requiring inter-communication by LAN. A second problem was a noticed inertia of the short ODL, especially when the scan rate is 10 Hz.

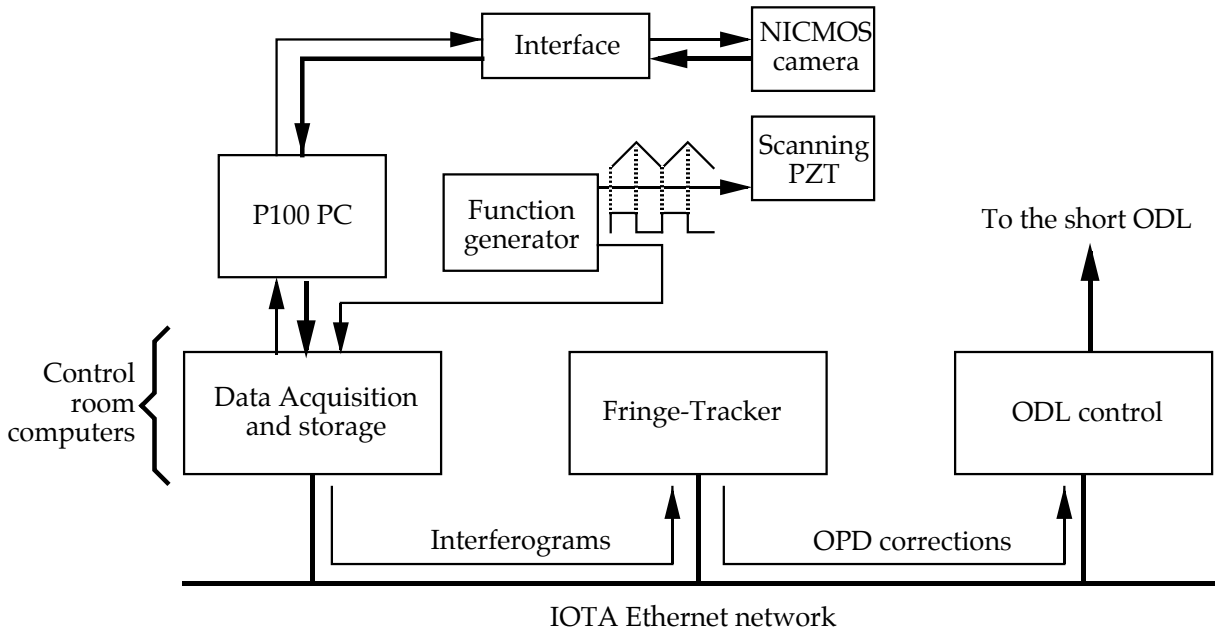

Figure 3. Diagram of the data flow in the fringe-tracking system tested on IOTA.

4. WHAT REMAINS TO BE DONE

4.1 PZT control

The scanning PZT is driven by a Physik Instrumente high-voltage amplifier featuring a function generator programmable by an external computer. All the parameters concerning the signal to generate are sent through a serial link to the amplifier. It will be therefore possible to reduce the scan range (i.e. slowing down the velocity of the scanning mirror while keeping the same sampling rate) to increase the fringe SNR if the differential piston is not too important. In this case, the OPD correction would be directly applied to the scanning PZT by adding an voltage offset to the driving signal. If the absolute mechanical range of the PZT does not allow such a correction, then an OPD offset is applied to the short ODL in order to bring back the PZT half-scan point (which should correspond to the null-OPD point) to the middle of its mechanical range. Moreover, the duty-cycle of the signal can be modified to increase the efficiency of the acquisition system.

Controlling the PZT requires a device to synchronize the NICMOS acquisition. In the current control system of IOTA, acquisitions by the Quadra are triggered by the leading edge of a TTL signal delivered by the external function generator. This TTL signal is synchronized on the triangle signal driving the PZT. For the fringe-tracker using PZT control, we wired an electronic temporal derivator giving a rectangle signal from the signal issued from the amplifier.

However, the control system of IOTA should be soon replaced by a VME chassis with PowerPC boards running under Wind-River's VxWorks, a real-time operating system[7]. Many improvements are expected from this new system which will control siderostat and ODL motion, tip-tilt correction and fringe acquisition. The implementation of a fringe-tracker will be easier thanks to a simplification of the communication between the processes.

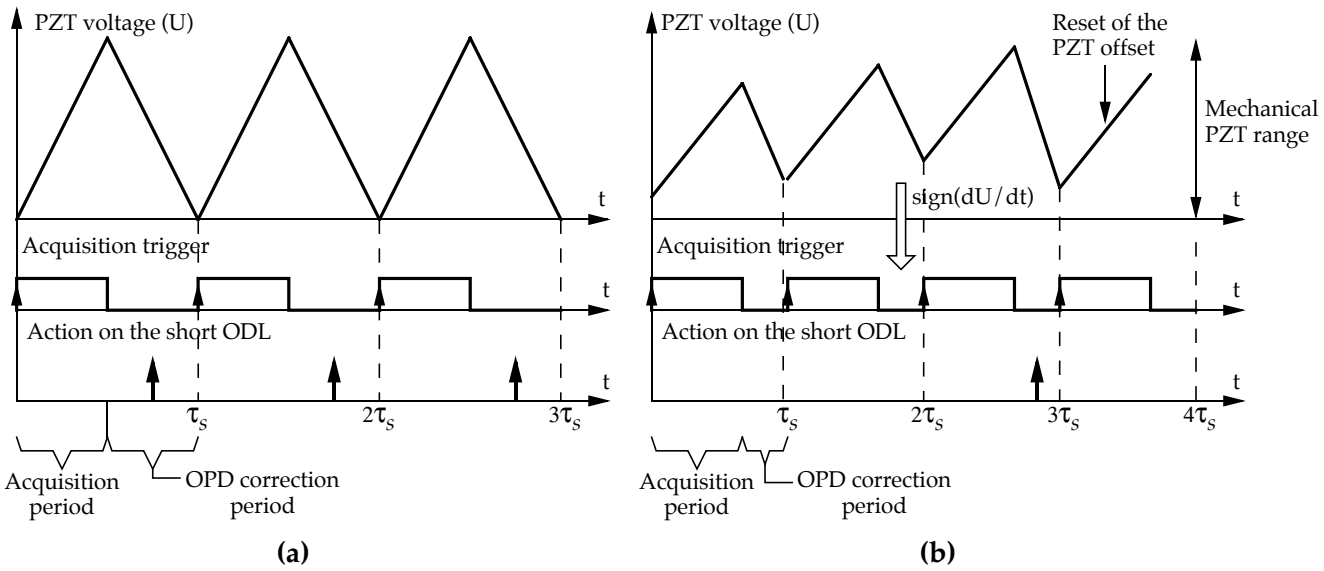

Figure 4. Chronograms of the voltage applied to the scanning PZT, the corresponding TTL signal for triggering NICMOS acquisitions, and the OPD correction on the short optical delay-line. (a): current situation ; (b): future system with PZT control by the fringe-tracker.

4.2 Prediction of the null-OPD point

Although the atmospheric differential piston is a random signal, its statistical properties derivate from Tatarski's models. Let ΔL_{dp} be the OPD component related to the differential piston for an interferometer characterized by a projected baseline B and apertures of diameter equal to D. From Taylor's hypothesis of a frozen turbulence moving at velocity V_a (with $\mathbf{B} = k.\mathbf{V}_a$), the power spectrum of ΔL_{dp} can be modelized by[8]:

$$\begin{cases} \mathcal{W}_{\Delta L_{dp}}(f) \propto f^{-2/3} & ; \quad \text{if } f < \dfrac{\mathrm{V}_a}{2\mathrm{B}} \\ \mathcal{W}_{\Delta L_{dp}}(f) \propto f^{-8/3} & ; \quad \text{if } \dfrac{\mathrm{V}_a}{2\mathrm{B}} \leq f < \dfrac{0,3.\mathrm{V}_a}{D} \\ \mathcal{W}_{\Delta L_{dp}}(f) \propto f^{-17/3} & ; \quad \text{if } f \geq \dfrac{0,3.\mathrm{V}_a}{D} \end{cases} \tag{1}$$

This power spectrum indicates that the temporal autocorrelation of ΔL_{dp} is not equal to zero for $\tau \neq 0$, i.e. ΔL_{dp} is not a white-noise. We assume that only the atmospheric differential piston contributes to significantly modify the position of the null-OPD point from one scan to the next one. The signal measured by the fringe-tracker is:

$$s[n] = \Delta L_{dp}[n] - \Delta L_{dp}[n-1] = \Delta L[n] - \Delta L_[n-1], \tag{2}$$

where n is an integer indexing the values of ΔL_{dp} at each scan. ΔL can be tracked from an origin by integrating s, yielding a temporal signal u. The fact that u, reflecting ΔL_{dp}, is temporally autocorrelated has been proved by measuring u at each scan the position of the null-OPD point with the first version of the fringe-tracker in open loop. The autocorrelation of u has then been computed yielding the result illustrated by Fig. . u can therefore be described by the auto-regressive (AR) model:

$$\tilde{u}[n+1] = \sum_{i=0}^{P-1} a[i].u[n-i], \tag{3}$$

where P is the order of the model. The issue is to determine the values of the AR model $\underline{a} = (a_0, ..., a_{P-1})^{\mathrm{T}}$ to minimize the mean quadratic error $< |u[n] - \tilde{u}[n]|^2 >$. Since no assumption regarding the stationarity of u can be made, especially for long observing periods where the turbulence conditions are changing, one should use an adaptive method to correct the AR model at each step, according to the actual value of u (determinated from the

algorithm described in part 2). We propose to use the weigthed recursive least square algorithm (WRLS), a familiar signal-processing method. At each scan indexed by n, the expected OPD is computed from the following equations:

$$\begin{cases} \underline{K}[n+1] = \underline{V}[n].\underline{u}[n].(\Lambda + \underline{u}[n]^{\mathrm{T}}.\underline{V}[n].\underline{u}[n])^{-1} \\ \underline{V}[n+1] = (\underline{1} - K[n+1].u[n]^{\mathrm{T}}).\underline{V}[n].\Lambda^{-1} \\ \underline{a}[n+1] = \underline{a}[n] + \underline{K}[n+1].(u[n+1] - \underline{a}[n]^{\mathrm{T}}.\underline{u}[n]) \end{cases} , \tag{4}$$

where $\underline{K}$ is a vector representing the adaptation gain (or "Kalman gain"), $\underline{V}$ is the covariance matrix, $\underline{1}$ is the identity matrix, $\underline{u}[n] = (u[n], ..., u[n-P-1])^{\mathrm{T}}$, and Λ is the "forgetting factor". Usually, $0.8 < \Lambda < 1$. This algorithm has already been proposed to improve fringe-tracking with GDT or RAFT[9]. Methods of the same type using ARMA models have been successfully used for adaptive optics[10]. In the case of IOTA, prediction could be employed for enhancing tip-tilt correction as well.

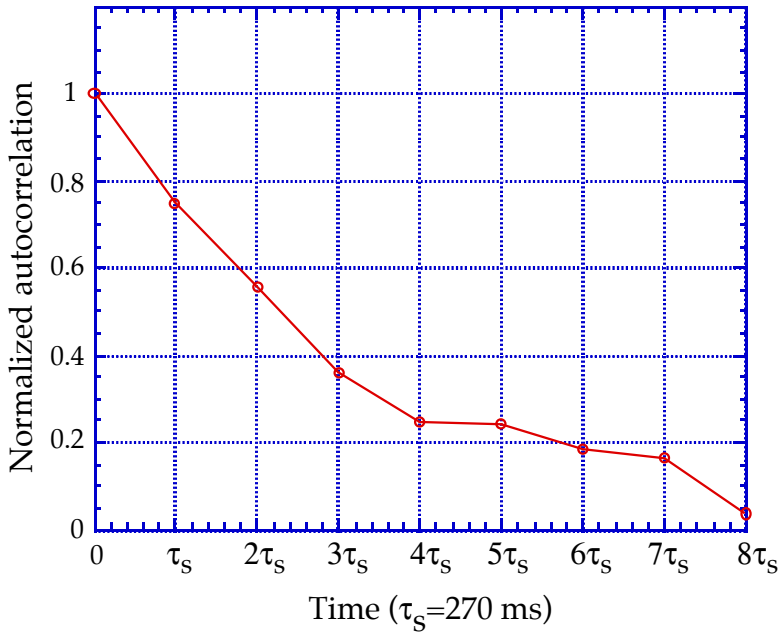

Figure 5. Normalized discrete temporal autocorrelation of the optical path difference drift (from a reference point) measured at IOTA with a 38 m baseline.

4.3 Fringe-tracking with FLUOR

The FLUOR recombiner has recently been improved and yields very accurate fringe contrast measurements. Its control system merely consists of a Macintosh G3 400 MHz computer in charge of NICMOS acquisition, scanning-PZT control (different from the one used on the beamsplitter table) and short-ODL control. The whole control software has been developed with National Instruments' LabVIEW graphic language. Thanks to this compact system and to the low scan rate used (2 Hz max.), a coherencer has easily been implemented on the FLUOR control system. It consists in finding the position of the centroid in the fringe packet. Each fringe packet has previously been filtered through a bandpass filter. Then the mean of the raw fringe packet is added to the filtered signal. The FLUOR coherencer includes an automatic fringe detector triggered when there is, in the interferogram, at least one peak which amplitude is larger than a preset threshold.

Since FLUOR is intended to be more and more used on IOTA, it would be interesting to try to improve the FLUOR coherencer by the algorithm described in part 2 and/or the prediction algorithm. Tests should be carried out during year 2000.

5. CONCLUSION

An automatic coherencing system for an infrared stellar interferometer can be made from a simple and fast algorithm. However, its implementation strongly depends on the characteristics of the existing control system. For IOTA, the coherencer for the beamsplitter table is expected to be always used during observation once the new VxWorks system will be installed only. Then, prediction algorithms may improve the performance of this coherencer. This might also benefit to the FLUOR coherencer which already exists. Closure-phase experiments at IOTA (scheduled for 2001) will certainly require this coherencing system.

6. ACKNOWLEDGEMENTS

We thank M. G. Lacasse for his help during the fringe-tracker experiments at IOTA. S. Morel is grateful to DGA-DRET (the scientific research office of the French Ministry of Defense) which funded him in 1999, and to NASA and the Smithsonian Institution for his 2000 fellowship.

7. REFERENCES

1. J. T. Armstrong, D. Mozurkewich, T. A. Pauls, A. R. Hajian, "Bootstrapping the NPOI: keeping long baselines in phase by tracking fringes on short baselines", *Proceedings SPIE, 'Astronomical Interferometry', 20-27 March 1998, Kona, Hawaii*, **3350**, pp. 461-466, 1998.
2. P. R. Lawson, "Group-delay tracking in optical stellar interferometry with the fast Fourier transform", *J. Opt. Soc. Am.* **A 12**, pp. 366-374, 1995.
3. L. Koechlin, P. R. Lawson, D. Mourard, A. Blazit, D. Bonneau, F. Morand, Ph. Stee, I.Tallon-Bosc, F.Vakili, "Dispersed fringe tracking with the multi-r_0 apertures of the Grand Interféromètre à 2 Télescopes", *Appl. Opt.* **35**, pp. 3002-3009, 1996.
4. M. Shao, D. H. Staelin, "Long-baseline optical interferometer for astrometry", *J. Opt. Soc. Am.* **67**, pp. 81-86, 1977.
5. V. Coudé du Foresto, G. Perrin, C. Ruilier, B. Mennesson, W. A. Traub, M. G. Lacasse, "FLUOR fibered instrument at the IOTA interferometer", *Proceedings SPIE, 'Astronomical Interferometry', 20-27 March 1998, Kona, Hawaii*, **3350**, pp. 856-863, 1999.
6. R. Millan-Gabet, F. P. Schloerb, W. A. Traub, N. P. Carleton, "A NICMOS3 camera for fringe detection at the IOTA interferometer", *Publ. Astron. Soc. Pac.* **111**, pp. 238-245, 1999.
7. W. A. Traub, N. P. Carleton, J. D. Bregman, M. K. Brewer, M. G. Lacasse, P. Maymounkov, R. Millan-Gabet, S. Morel, C. Papaliolios, M. R. Pearlman, I. Porro, F. P. Schloerb, "The third telescope project at the IOTA interferometer", *Proceedings SPIE, 'Interferometry in Optical Astronomy', 27-31 March 2000, Munich, Germany*, **4006**, in preparation.
8. G. Perrin, "Correction of the "piston effect" in optical astronomical interferometry. I. Modulus and phase gradient of the visibility function restoration", *Astron. & Astroph. Suppl. Ser.* **121**, pp. 553-568, 1997.
9. S. Morel, L. Koechlin, "Fringe tracking using a priori information on the optical path difference drift", *Proceedings SPIE, 'Astronomical Interferometry', 20-27 March 1998, Kona, Hawaii*, **3350**, pp. 1057-1064, 1998.
10. C. Dessenne, P.-Y. Madec, G. Rousset, "Optimization of a predictive controller for closed-loop adaptive optics", *Appl. Opt.* **37**, pp. 4623-4633, 1998.